

# We are IntechOpen, the world's leading publisher of Open Access books Built by scientists, for scientists

5,500

Open access books available

135,000

International authors and editors

165M

Downloads

Our authors are among the

154

Countries delivered to

TOP 1%

most cited scientists

12.2%

Contributors from top 500 universities



WEB OF SCIENCE™

Selection of our books indexed in the Book Citation Index  
in Web of Science™ Core Collection (BKCI)

Interested in publishing with us?  
Contact [book.department@intechopen.com](mailto:book.department@intechopen.com)

Numbers displayed above are based on latest data collected.  
For more information visit [www.intechopen.com](http://www.intechopen.com)



# Quantum Chemical Investigations of Structural Parameters of PVDF-based Organic Ferroelectric Materials

A. Cuán<sup>1</sup>, E. Ortiz<sup>1</sup>, L. Noreña<sup>1</sup>, C. M. Cortés-Romero<sup>1</sup>, and Q. Wang<sup>2</sup>

<sup>1</sup>*Basic Science Department and Materials Department, Metropolitan Autonomous University-Azcapotzalco. Av. San Pablo 180, Col. Reynosa Tamaulipas, 02200*

<sup>2</sup>*Department of Materials Science and Engineering. The Pennsylvania State University, University Park PA 16802,*

<sup>1</sup>*México D.F.*

<sup>2</sup>*USA*

## 1. Introduction

Poly(vinylidene fluoride)-based polymers have been the research focus of many groups due to the discovery of piezoelectricity in this material, by Kawai et al in 1969. PVDF is constituted by sequential  $[-(\text{CH}_2\text{-CF}_2)_n-]$  chains and known as the first crystalline organic ferroelectric material, which makes it critically important, since there exist only few classes of materials with ferroelectric properties, such as perovskite-type  $\text{ABO}_3$  metal oxides ( $\text{BaTiO}_3$ ,  $\text{PbTiO}_3$ , or  $\text{KNbO}_3$ ) (Sakashita et al, 1987). Drawbacks of the latter material are related to its heavy weight, brittleness and substantial costs of device manufacturing. Thus, the organic ferroelectrics materials arise as suitable alternative to metal oxides because of better prospective technological applications.

PVDF-based polymers have polymorph properties and at least five experimentally characterized crystal phases, namely, the all-trans ( $T_p$ ) planar zigzag  $\beta$ -phase,  $TG_a$  and  $TG_p$ , (where G denotes the gauche form), the  $\alpha$ - and  $\delta$ -phases, and the  $T_3GT_3G'$  ( $T_3G_a$ ,  $T_3G_p$ )  $\gamma$ - and  $\varepsilon$ -phases (Lovinger, 1982; Broahurst, 1978). Nevertheless, among these phases, only the all-trans conformation (or  $\beta$ -phase) exhibits ferroelectric behavior. The  $T_p$  conformation of the all-trans phase, has a highly polarized backbone with the highest spontaneous polarization in a unit crystal cell (Jungnickel, 1999). This spontaneous polarization gives the special ferroelectric properties, leading to a broad potential of application in several new-technology electronics, such as in sensors, transducers, energy storage devices, communications and microphones (Kawai, 1969; Lovinger, 1983; Jungnickel, 1999; Lando et al., 1966; Farmer et al., 1972; Hasegawa et al., 1972; Karasawa & Goddard, 1992; Tashiro et al., 1995; Nalwa, 1995; Lang, 2006; Wang et al., 1988). A drawback, however, of the synthesized  $\beta$ -PVDF pure material, is that the maximum crystallinity reached is 50%, which results in lower polar properties than those of pure  $T_p$  phase, if formed.

Some applications currently under development include artificial muscles and harnessing energy from sea waves. The ferroelectric properties of PVDF can be enhanced by the introduction of trifluoroethylene, TrFE, as comonomer. P(VDF-TrFE) exhibits ferroelectric

properties at TrFE contents between 50 and 85 mole percent (Lu et al., 2006). At a specific temperature, the Curie temperature, P(VDF-TrFE) copolymers show a conformational and phase transformation, from ferroelectric to paraelectric. The Curie temperature depends on the copolymer composition and at this temperature the PVDF-based materials show some of the highest dielectric constants of any organic polymer, resulting from large crystalline polar domains. However, for energy storage applications, as in capacitors, is more convenient a relatively high dielectric constant at room temperature and a smaller remnant polarization (Lu et al., 2006), that can be accomplished by reducing the crystal domain size through high energy radiation or by the introduction of a third monomer, such as chlorotrifluoroethylene P(VDF-CTFE). Experimental results indicate that the crystalline domain in P(VDF-TrFE)s and its size play an important role in the dielectric response (Zhang et al., Lovinger, 1985, Daudin & Dubus, 1987; Tashiro et al, 1988; Furukawa, 1990; Casalini & Roland, 2001; Gao & Scheinbeim, 2000; Casalini & Roland, 2001).

Both, experimental and theoretical works have been devoted to the study of PVDF-based materials unique piezoelectric, pyroelectric, ferroelectric, electro-acoustic and nonlinear optical properties (Jungnickel, 1999; Lando et al., 1966; Farmer et al., 1972; Hasegawa et al., 1972; Karasawa & Goddard, 1992; Tashiro et al., 1995; Nalwa, 1995; Lang, 2006; Wang et al., 1988). Common dielectric materials may become polarized under an applied electrical field, whereas ferroelectric materials may become spontaneously polarized. Piezoelectric materials can transform a mechanical movement into an electric signal and vice versa. On the other hand, electro-acoustic materials can transform an acoustic wave into an electric signal and vice versa.

The density functional theory (DFT) is a powerful tool for both, elucidation of and understanding the PVDF-based materials structure-property relationships. The relative accuracy of DFT is comparable to that of traditional *ab-initio* molecular orbital methods. However, the computational requirements of DFT calculations are much less demanding, allowing us to efficiently study the large systems needed for the realistic modeling of PVDF-based materials. Theoretical and experimental studies can greatly aid our atomic-level understanding of ferroelectric properties. Herein, we briefly describe the technical details of DFT methodologies and the factors that influence the accuracy of the results. Examples of DFT applied to PVDF-based materials features, like phase transition and their related electronic properties, are presented, demonstrating the important role DFT plays in the study of these kinds of materials.

Theoretical investigations for the aforementioned materials are presented and discussed within this manuscript. Molecular models commonly employed, methods applied to these materials, and results currently obtained for the energetics and structures corresponding to the different conformations, i.e., the changes in the molecular arrangement associated to  $T_p$ ,  $TG_a$  or  $TG_p$  conformations, are also presented. Properties such as the charge polarization and the dipole moment increment produced by enlarging the chain components that actually confer the ferroelectric properties are reviewed as well.

## 2. Quantum theory as an analytical chemistry tool

The complete characterization of any mechanism, phase stability or phase transitions and its structure-property relationships is a huge task, nevertheless, considering its potential economic and environmental impact in industry, it is clear that deeper knowledge in it would be of great benefit.

The rational optimization and design of a PVDF-based material requires fundamental information concerning the structure and function of these materials under ideal conditions. Quantum mechanics (QM) methods, which we also denote as QCC (Quantum Chemical Calculations) can provide valuable information about the electronic and structural phase transitions for several polymer backbones giving an insight into structure-property relationships, which are not yet completely elucidated (Broahurst et al. 1978; Jungnickel, 1999; Tashiro et al., 1988; Casalini & Roland, 2001; Gao & Scheinbeim, 2000; Casalini & Roland, 2002; Nicholas, 1997; Nicholas et al., 1991; Gómez-Zaravaglia & Fausto, 2004; Teunissen et al., 1994; Sierra, 1993; Evleth et al., 1994; Das & Whittenburg, 1999). Therefore, the first principles-based materials models are helpful for the design of materials with improved properties. In this concern, QCC together with experimental techniques have reached widespread application as a tool for characterization of a reactive system and spectra modeling (Nicholas, 1997).

The experimental spectroscopic results are often confronted with theoretical calculations in which the vibrational frequencies are computed and afterwards analyzing the corresponding mode in order to reproduce the model molecule characterization (Nicholas et al., 1991; Gómez-Zaravaglia & Fausto, 2004). Moreover, it is possible to make a model of a solid crystalline system or instead be treated as a molecule, depending on the properties that we wish to obtain.

### **2.1 Quantum mechanics methods applied to PVDF-based materials**

The QM methods offer the opportunity to study electronic structure at the microscopic level. Within the QCC methods there are different approximations levels, i.e., the Moller-Plesset (MP2) and Configuration Interaction (CI), which are some of the most accurate and involve electronic correlation. The required time for running a calculation is about  $N^5$ , where  $N$  is the basis set employed for the atomic orbital description (Teunissen, 1994). Other approximations such as the Hartree-Fock (HF) ( $N^4$ ) and the Density Functional (DFT) ( $N^3$ ) level of theory require shorter computing time (Sierra, 1993; Evleth et al., 1994) with the possibility of applying them to a larger system size, having less accuracy but similar phenomena description to those of MP2 and CI, (further details are reported in Das & Whittenburg in 1999). The DFT offer some computing time advantages and a quantitative characterization of electronic-structures properties and in order to gain insight in these phenomena it is necessary to build predictive, then the first principles-based materials models. DFT methodology results are helpful for the design of PVDF-based materials.

### **2.2 Molecular models commonly employed in QCC**

Crystalline or semi-crystalline molecular modeling can be of different complexity level, depending on the target of the study. Periodic boundary conditions or finite models are commonly employed in QCC. In this concern, some investigations have been reported with both models as described further on. In addition, QCC contributes to predict the energetic and structures corresponding to the different conformations, as their relationship to charge polarization and to dipole moment enhancement, that in molecular design, can be related to the ferroelectric properties of PVDF-based materials.

Using periodic boundary conditions (Chun-gang et al., 2003) from first-principles, the band structure approach with full-potential linear augmented-plane-wave method (FLAPW)

(Blaha, 1997) can be applied to the study of PVDF and P(VDF-TrFE) and the band gap and symmetries can be correlated in line with experimental photoemission data. As a reminder, P(VDF-TrFE) stands for poly-vinylidene fluoride-trifluoroethylene copolymers. They also found that the interactions between different PVDF chains are rather weak, which reflects clearly the quasi-one-dimensional nature of the system. Concerning the electronic structure of P(TrFE), results indicated that replacing  $-(\text{CH}_2-\text{CF}_2)-$  by  $-(\text{CHF}-\text{CF}_2)-$  does not change major features of the band structure.

Other contribution using periodic conditions has been reported (Haibin Su et al. 2004). These authors used DFT pseudopotential code SeqQuest (Schultz, 2002; Feibelman, 1987) which makes use of Gaussian basis sets to study static and dynamical mechanical properties of PVDF and its copolymer with trifluoroethylene (TrFE). With this methodology, they found that conformations with T and G bonds are energetically favorable for large interchain separations if compared to all-T structures. These results are in line with the experimental observation that samples irradiated with high-energy electrons favor  $T_3G$  nonpolar conformations. With this methodology it is also possible to obtain the crystal cohesive energy ( $E_{\text{coh}}$ ) and energy stabilization of the different conformation or phases.

On the other hand, other research groups, (Nicholas et al., 2006) have performed DFT calculations *via* the ABINIT software package with periodic boundary conditions employing Perdew BurkeErnzerhof generalized-gradient approximation (GGA) (Perdew, 1996) and pseudopotentials (Rappe, 1990). Together with this strategy they also used the OPIUM code which led to a full reproduction of the structure and NMR and FTIR vibrational frequencies of the  $\alpha$ -PVDF phase. With these results, they contributed to the understanding of those mode ambiguities founded experimentally (Makarevich & Nikitin, 1965; Wentink et al., 1961; Cortili & Zerbi, 1967; Kobayashi et al., 1975).

In the case of finite models that are treated as molecules (Das et al., 1999), the DFT methodology with *ab-initio* methods implemented in the Gaussian 94 software package help in geometric structure, vibrational frequency, dipole moment and singlet-triplet energy separation of  $\text{CH}_2$ , CHF,  $\text{CF}_2$ ,  $\text{CCl}_2$  and  $\text{CBr}_2$  studies, using B3LYP, B3P86 and B3PW91 hybrid density functionals. For the case of the methylene group ( $\text{CH}_2$ ), the density functionals predict the equilibrium C-H bond length, the H-C-H bond angle and the vibrational frequency up to an accuracy level comparable to high-level *ab initio* methods. However, they found that only the B3LYP functional produces reasonable singlet-triplet energy separation. Estimates of the singlet-triplet energy separation of CHF and  $\text{CF}_2$  indicate B3LYP functional produces better agreement with experimental data than B3P86 or B3PW91.

Another contribution was made by (Zhi-Yin, 2006). They reported a study of the internal rotation, geometry, energy, vibrational spectra, dipole moments and molecular polarizabilities of PVDF in  $\alpha$ - and  $\beta$ -chain models employing the density functional theory at B3PW91/6-31G(d) level. They found the effects of chain length and monomer inversion defects on the electric properties and vibrational spectra. They also reported that the average distance between adjacent monomer units in the  $\beta$ -PVDF is 2.567 Å and that the energy difference between the  $\alpha$ - and  $\beta$ -chains is about 10 kJ/mol per monomer unit. They found that the dipole moment is also affected by chain curvature and by defect concentration and that the chain length and defects will not significantly affect the polarizability. Those are some of the reported results presented about this topic, as can be seen, depending on the model and methodology, we can obtain different structural and electronic properties relationships. Then, insight has been gained from the QCC literature in which both periodic and finite models have been proposed with considerably good acceptance.

### 2.3 When do models correctly describe the PVDF-based materials?

There is not a gradual development of quantum chemical models or methodologies applied to PVDF-based materials, which for instance occurred in the case of other macro systems, such as zeolite catalysts (Cuán & Cortés-Romero, 2010). The reason lies on the current development of the software and hardware that, unlike for zeolite-based materials, is not a limitation anymore for PVDF-based materials. Researchers are applying all the possible QM tools to the molecular design of this polymer due to the complexity and importance of this phenomenon.

So far, the crystalline or semi-crystalline molecular modeling of these materials can be of different level of complexity depending on the purpose. Periodic or finite models give valuable information, but the model employed and the correct description will be in terms of some factors, such as the properties to be estimated or reproduced, geometrical description, computational resources (software and hardware) and quality of the theoretical approximation. Nevertheless, in many cases a simple molecular model can give valuable information, as it will be discussed below.

## 3. Test case of PVDF-based materials using finite models

### 3.1 Model representation

Five different-length chain molecules were studied for PVDF,  $H-(CH_2-CF_2)_x-H$ , where  $x=1,2,4,6$  for the four different PVDF molecules conformations, namely, I= $T_p$ , II= $TG_a$ , III= $TG_p$  and IV = $T_3G$ , *vide* Figure 1(a), and for the PVDF-based materials PVDF-TrFE and

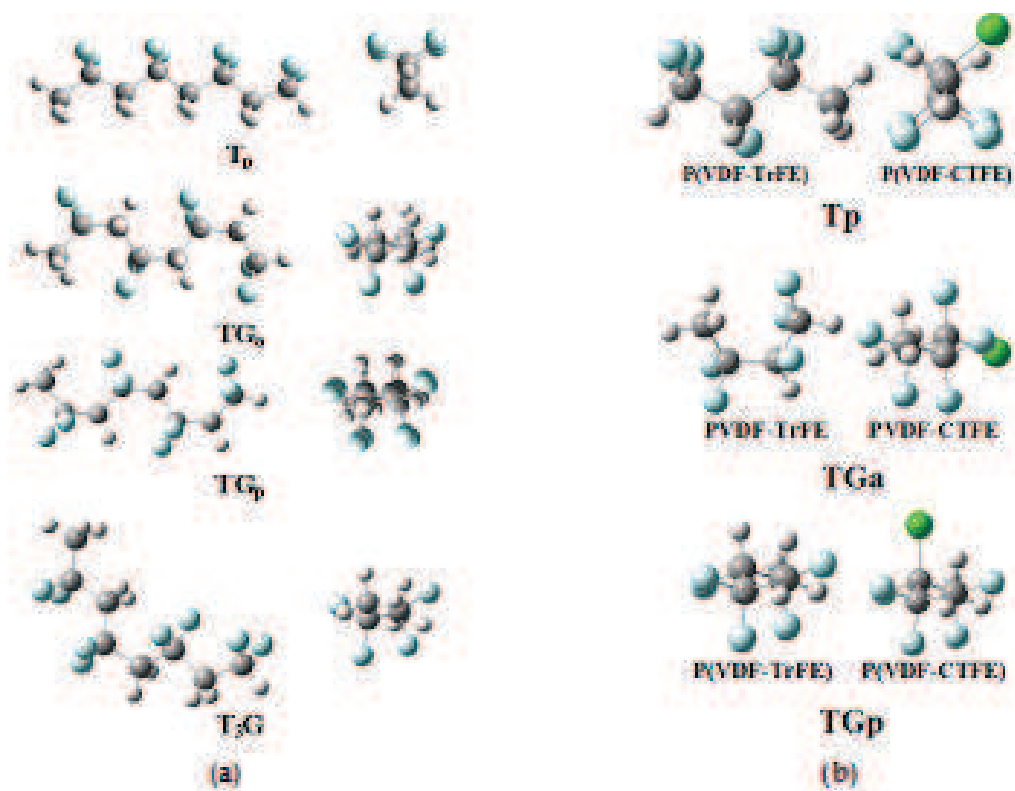


Fig. 1. Structural representation for the different PVDF conformers, namely,  $T_p$ ,  $TG_a$ ,  $TG_p$  and  $T_3G$ . Fluorine atoms are in blue, carbon atoms are in grey and hydrogen atoms are in white. a) PVDF b) P(VDF-TrFE) and P(VDF-CTFE).

PVDF-CTFE, only the three representative conformations were taken from PVDF and calculated, they are denoted as  $T_p$ ,  $TG_a$  and  $TG_p$  phases, *vide* Figure 1(b). T means all-T, TG indicates  $TGTG'$  and  $T_3G$  means  $TTTGTG'$ , where T indicates trans and G means gauche conformation and the subindexes p and a correspond to polar phases with parallel dipoles and nonpolar phases with antiparallel dipole moments, respectively.

### 3.2 Stepwise theoretical methodology used

The electronic structure study includes all-electrons within the Kohn-Sham implementation of the Density Functional Theory (DFT). The level of theory used in this work corresponds to the non-local hybrid functional developed by Becke, Lee-Yang-Parr (B3LYP) (Becke, 1993; Lee et al., 1988) whereas the Kohn-Sham orbitals are represented by a triple- $\zeta$  numerical with double polarized functions (d,p) plus one diffuse basis set; implemented in the Gaussian 03 code, this methodology was carried out within finite models. The electrostatic potential method was used for the charge calculation (ESP) (Brent, 1990). The Electrostatic Potential (ESP) charge calculation algorithm was chosen because it has no basis set dependence. Geometry optimization calculations were carried out for all the involved systems using the Berny algorithm. The Threshold convergence criterion was  $10^{-6}$  hartrees for the energy, 0.000450 for the Maximum Force and 0.001800 for the Maximum Displacement.

### 3.3 Active phase formation

In order to understand the differences among the chemical and electrical properties of PVDF with respect to the P(VDF-TrFE) and P(VDF-CTFE) materials, we performed the torsion of the dihedral angle of representative two monomer units, i. e.,  $n_r=4$ , where  $n$  is the total number of carbon atoms in the structure, *vide* Figure 2. Following the dihedral angle torsion of the G -to- T geometry transformation, the potential energy surface (PES) gives the relative energies and structural changes among them. Figure 2 shows that the  $TG_a$ ,  $TG_p$  and  $T_p$  are stable geometric conformations for all the materials, because all of them are situated at minimum positions within the PES. We shall bear in mind that the molecular energy computed in this simplified model is far away from that of the real crystal (formed by large domains); nevertheless, computing simulations are consistent with available experimental observations (Wang et al., 2006; Ortiz et al., 2009; Ortiz et al., 2010). According to Figure 2, it is possible to observe that for all the materials, the TG phases are energetically more stable than the  $T_p$  phase, and that the PVDF-PES profile shows a symmetric curve distribution, *vide* Figure 2(a); which is mostly due to the symmetric disposition of fluorine substituents. In the P(VDF-TrFE)-PES and the P(VDF-CTFE)-PES this even distribution is lost, because the addition of substituents to the PVDF, such as fluorine and chlorine, *vide* Figure 2(b) and (c). Then, according to Figure 2, to reach the  $T_p$  conformation requires an energy supply for all the three cases. *Barrier 2 (Barr2)* indicates the amount of energy required to reach  $T_p$  from  $TG_p$ ; approximately 4 kcal/mol for PVDF, 4.86 kcal/mol for P(VDF-TrFE) and 3.05 kcal/mol for P(VDF-CTFE) (*vide* Table 1). For the PVDF case, the order of the energy difference is in agreement with that reported elsewhere (Wang et al., 2006; Ortiz et al., 2010). On the other hand, *Barrier 3 (Barr3)* indicates the amount of energy required to reach  $T_p$  from  $TG_a$  being around 2.1, 3.5, and 1.0 kcal/mol following the same order mentioned before. Now, *Barrier 1 (Barr1)* represents the amount of energy required to reach  $TG_p$  from  $TG_a$  being around 3.9, 4.0, 1.8 kcal/mol, keeping the same ordering. Based on the computed results, the

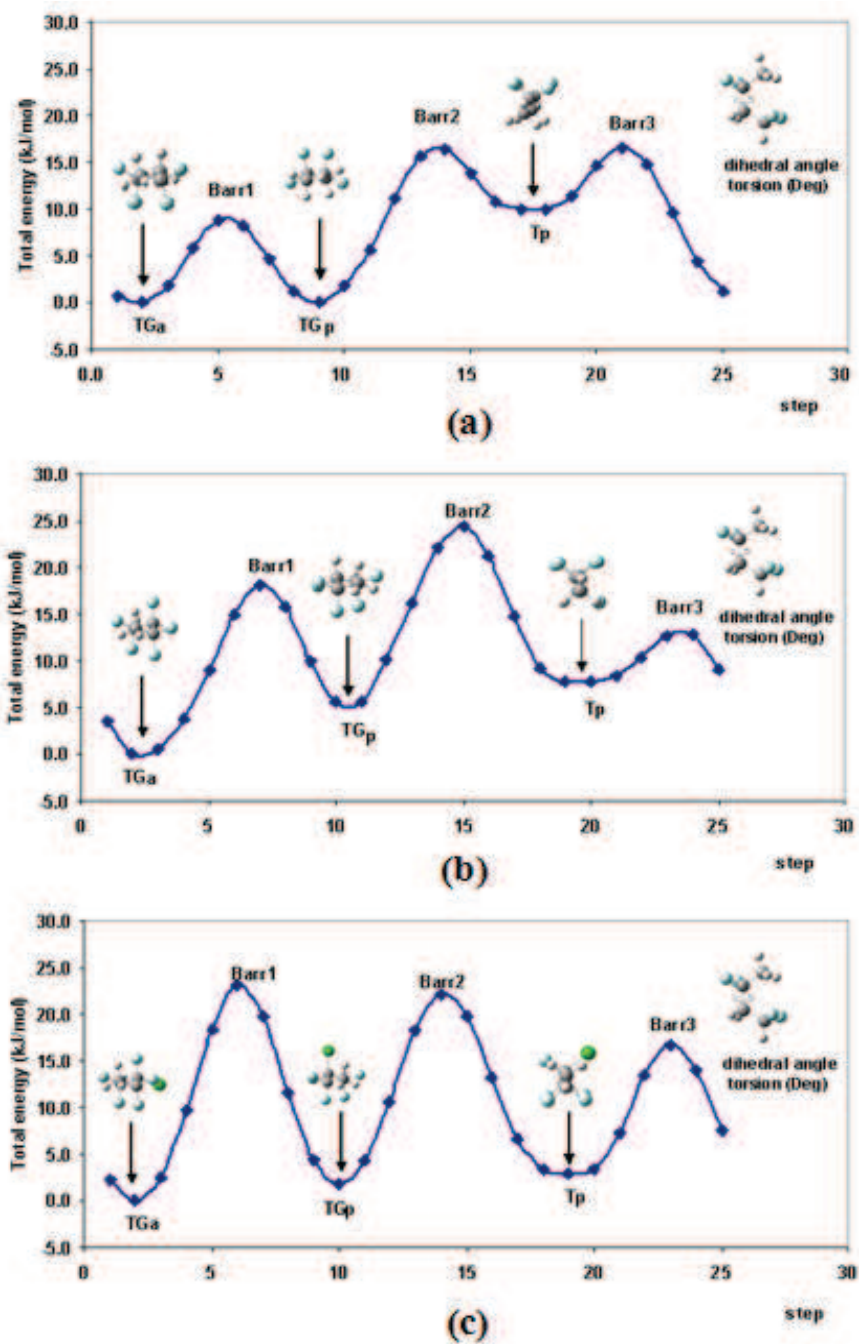


Fig. 2. Graphical representation of the PES for the dihedral angle torsion showed on the right side of the picture. This graph displays the energy associated to the different model structural conformations,  $TG_a$ ,  $TG_p$  and  $T_p$  of the different materials: (a) PVDF, (b) P(VDF-TrFE) and (c) P(VDF-CTFE).

energy barrier for converting the  $TG_a$  into the  $TG_p$  structural conformation is half of the energy required to reach the  $T_p$  structural conformation for the PVDF material, as it can be observed in Figure 2, while for the P(VDF-TrFE) increases almost one time and for the P(VDF-CTFE) there is no significant difference. The situation is not the same when  $Barr2$  and  $Barr3$  are compared, here for converting the  $TG_a$  into the  $TG_p$  with respect to reach the  $T_p$  conformation, for the case of P(VDF-TrFE) the amount of energy diminished three times,

if compared with PVDF, which means that this process would occur more easily. Although for P(VDFCTFE) the energy required increases again one and a half times.

The analysis of the energy differences among the structural phases involves looking at the minima points along the PES for the different materials conformations, as follows. For PVDF, TGa and TGp have a similar energy level, *vide* Figure 2 (a), while the energy difference between them and the Tp conformer is about 2.3 kcal/mol. For P(VDF-TrFE), according to Figure 2 (b), TGa is more stable than TGp by 1.46 kcal/mol; the Tp conformer is placed 1.92 kcal/mol above than TGa and only 0.5 kcal/mol above than TGp. Note that for this material it would be easier to reach the Tp phase from TGa, due to the considerable reduction of the rotational barrier, with respect to the others, *vide* Table 1. Analyzing the graphical representation in Figure 2(c), but now for P(VDF-CTFE), all the conformations, namely, TGa, TGp and Tp have a similar energy level, with less than 1 kcal/mol difference among them. These results mean, that for P(VDF-CTFE), the Tp phase becomes almost as stable as the TGa or TGp phases, although the rotational energy barrier for reaching the Tp conformation is larger than for the other systems; but once the energetic barrier may be overcome, a stable structure is obtained. These structural conformations are related with a corresponding phase in the crystal. Then, the active phase formation could be correlated to the conformational geometry and the rotational dihedral angle during the formation of Tp phase. The rotational barriers found for each different composition affect both the higher mobility of the C-F dipoles and the structural rearrangement of the systems which actually produce the differences in polymers properties and, hence, applications. Somehow, the rotational barriers and its energy level are a function of the fluorine composition and the degree of contamination (chlorine content) which is expected by the presence of this halogen.

System	Phase	$\Delta E_{Ph-Tr}$ Kcal/mol (kJmol)	$\Delta E$ Kcal/mol (kJmol)	$\Delta E_{H-L}$ (eV)	Dipole (D)
PVDF	Tp	2.373 (9.92)	<i>Barr1</i> 3.929 (16.44)	9.24	4.68
	TGa	0.000 (0.00)	<i>Barr2</i> 3.954 (16.55)	9.57	2.37
	TGp	0.020 (0.08)	<i>Barr3</i> 2.095 (8.77)	9.56	2.55
PVDF-TrFE	Tp	1.924 (8.05)	<i>Barr1</i> 3.992 (16.70)	8.32	2.54
	TGa	0.000 (0.00)	<i>Barr2</i> 4.862 (20.34)	8.43	1.65
	TGp	1.457 (6.10)	<i>Barr3</i> 3.501 (14.65)	8.36	2.30
PVDF-CTFE	Tp	0.698 (2.92)	<i>Barr1</i> 1.777 (7.44)	9.07	3.65
	TGa	0.000 (0.00)	<i>Barr2</i> 3.050 (12.76)	9.43	1.24
	TGp	0.435 (1.82)	<i>Barr3</i> 0.608 (2.54)	9.28	3.35

$$\Delta E_{Ph-Tr} = E(\text{phase TGa}) - E(\text{corresponded - phase}), \text{ i.e., Tp or TGp}$$

$$\Delta E_{H-L} = |E_{HOMO} - E_{LUMO}|$$

$$Barr1 = E(\text{Phase Tp}) - E(\text{Phase TGa})$$

$$Barr2 = E(\text{Phase Tp}) - E(\text{Phase TGp})$$

$$Barr3 = E(\text{Phase TGp}) - E(\text{Phase TGa})$$

$$\mu = \text{Debye}$$

Table 1. Phase transition energy ( $\Delta E_{Ph-Tr}$ ), Rotational barrier ( $\Delta E$ ), HOMO-LUMO GAP ( $\Delta E_{H-L}$ ) and Dipole moment ( $\mu$ ) for the representative two monomer units of PVDF, P(VDF-TrFE) and P(VDF-CTFE).

### 3.4 Physicochemical and electrical properties

PVDF material is the base of the organic ferroelectric material and although  $\beta$ - structure serves well as a simple model for basic understanding of the polar nature of ferroelectric polymer crystal, it is necessary to study the electronic-structure relationship and the behavior of these polymers when the environment changes, i.e., variation in VDF-to-copolymer concentration. We currently used five different-length chain molecules as a model of  $H-(CH_2-CF_2)_x-H$ , where  $x = 1, 2, 4, 6$  for the four different PVDF conformations, namely,  $T_p$ ,  $TG_a$ ,  $TG_p$  and  $T_3G$  and compare with PVDF-based materials electronic properties.

#### 3.4.1 PVDF material case

The analysis of the differences among the structural changes obtained along the PES in Figure 2 (a) leads to the values in Table 2 where some electronic properties and their

No. of C Atoms $n_r$	Length L (Å)	$E_{HOMO}$ (eV)	$E_{LUMO}$ (eV)	$\Delta E^a$ (eV)	Dipole (D)
			<b><math>T_p</math></b>		
2	3.30	-9.63	0.08	9.72	2.52
4	5.62	-9.24	-0.33	8.91	4.68
6	8.17	-9.08	-0.58	8.50	6.74
8	10.68	-8.99	-0.75	8.25	8.76
12	15.63	-8.93	-0.95	7.98	12.70
			<b><math>TG_a</math></b>		
2	3.30	-9.63	0.08	9.72	2.52
4	5.25	-9.57	-0.19	9.38	2.37
6	7.62	-9.47	-0.37	9.11	4.30
8	9.86	-9.41	-0.46	8.95	5.04
12	14.43	-9.30	-0.57	8.72	7.97
			<b><math>TG_p</math></b>		
2	3.30	-9.63	0.08	9.72	2.52
4	5.26	-9.56	-0.07	9.49	2.55
6	7.62	-9.48	-0.48	9.01	4.08
8	9.86	-9.42	-0.57	8.84	4.73
12	14.43	-9.31	-0.70	8.605	7.57
			<b><math>T_3G</math></b>		
2	3.30	-9.63	0.08	9.72	2.52
4	5.26	-9.57	-0.19	9.38	2.36
6	6.75	-9.38	-0.49	8.89	3.32
8	9.90	-9.19	-0.56	8.632	3.64

<sup>a</sup>  $\Delta E = E_{LUMO} - E_{HOMO}$  (eV)

Table 2. Length chains (carbon atom number) for the different PVDF structural conformations and their electronic properties: HOMO energy, LUMO energy, <sup>a</sup>  $\Delta E = E_{LUMO} - E_{HOMO}$  and dipole moment.

corresponding parameters are presented. Considering only two monomer units, i. e.,  $n_r=4$ , where  $n$  is the total number of carbon atoms in the structure, the computed results indicate that the dipole moment of the  $T_p$  conformation is approximately 40% higher than that of the rest of the structural conformations ( $TG_a$ ,  $TG_p$  and  $T_3G$ ), *vide* Table 2. The dipole moment of the different conformations is presented in Figure 3. The blue line corresponds to the dipole moment variation depending on the chain length of the  $T_p$  conformation. Similarly, the green line corresponds to the  $TG$  (a or p) conformation and the orange line corresponds to the  $T_3G$  phase. In general, the picture shows that the dipole moment increases as the length of the carbon chain increases. The  $T_p$  conformation exhibits the larger increase in the dipole moment. The  $TG$  structural conformation shows an intermediate increase whereas the  $T_3G$  conformational phase has the lowest one. The dipole moment increase for  $T_p$  is about 40% stronger than the  $TG$ 's conformations and 55% stronger than the  $T_3G$  conformation. This means that the structural arrangement of the  $T_p$  phase promotes an increase in the polarity of the system, as already known. The charge polarization can also be obtained (*vide* Figure 4), where the positive and negative ESP charges in the  $T_p$  conformation are perfectly ordered at the outside part of the molecule. The  $TG$ 's and  $T_3G$  conformational systems do not show the same split charge distribution.

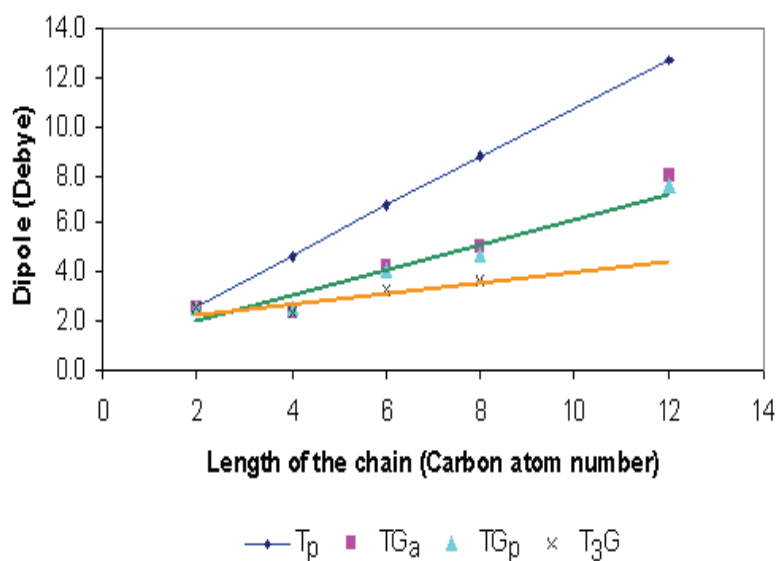


Fig. 3. Dipole moment trend (in Debye) for the different PVDF structural conformations. In blue for  $T_p$ , in green for  $TG_a$  and  $TG_p$  and in orange for  $T_3G$ .

Hence, the dipole variation and the charge polarization of the  $T_p$  system are characteristic of a ferroelectric material; they together act to form an electric dipole moment even in the absence of an external electrical field, as it is currently demonstrated. This behavior is a result of a change in the phase structure. Moreover, the simple molecular model in Figure 2 shows that the energy barriers among the different structural conformations are not too high to avoid switching among them with a relatively low energy supply.

Figures 5 and 6 show the electronic states distribution of the valence band and the conduction band for the  $T_p$  and  $TG_p$  conformers, respectively. We can observe that the band gap between the valence and the conduction bands decreases as the total number of carbon atoms increases; being shorter in the  $T_p$  conformer than in the  $TG_p$  conformer. The number of empty molecular orbitals under the Fermi level increases as the length of the chain also

increases. Therefore, the  $|\text{HOMO-LUMO}|$  energy difference also exhibits a decrease, being highly notorious for the  $T_p$  conformer, from 9.72 eV to 7.98 eV but they correspond to a simplified model, which tendency is to decrease with the system is enlarged (*vide* Table 2), the experimental value reported is about 6.5 eV (Choi Jaewu et al., 1998). In the  $T_p$  conformer there is a noticeable increase of the empty states under the Fermi level. Although, the reduction in the  $|\text{HOMO-LUMO}|$  band gap is low, whereas the conduction band lies sufficiently low for rendering a negative band gap value, corresponding to a semimetal behavior. However, the spontaneous polarization of the  $\beta$ -phase might be associated to a higher sheet carrier density with respect to the bulk.

Then, we can conclude partially that the changes in the molecular arrangement associated to  $T_p$ ,  $TG_a$  or  $TG_p$  and  $T_3G$  conformations lead to significant changes in shape and electrical-chemical properties. A larger dipole moment and spatial charge polarization were obtained for the all-trans  $T_p$  molecular structure, which can be obtained by accumulative motion of the neighboring groups, through large-scale T-G conformational changes. The dipole moment increase and the charge polarization in the  $T_p$  system are characteristics of a ferroelectric material. These contribute to form an electric dipole moment, even in the absence of an external electrical field.

### 3.4.2 PVDF-based materials

Now, in order to get insight and better understanding of the electronic-structure relationships and changes in behavior, leading towards enhanced ferroelectric properties produced by environment changes, we have also studied P(VDF-TrFE) and P(VDF-CTFE) copolymers and compared the differences or similitudes to the pure PVDF.

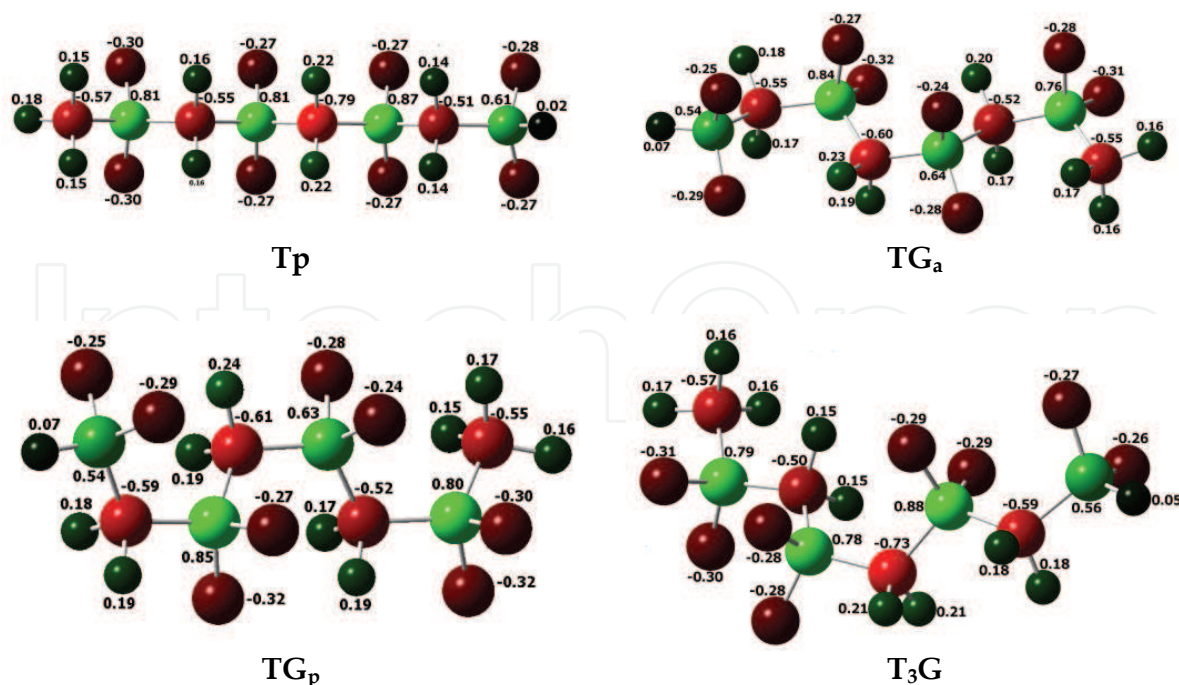


Fig. 4. ESP charge representation for  $T_p$ ,  $TG_a$ ,  $TG_p$  and  $T_3G$ . Negative charge values are in red, positive charge values are in dark green and the larger positive charges are depicted in light green.

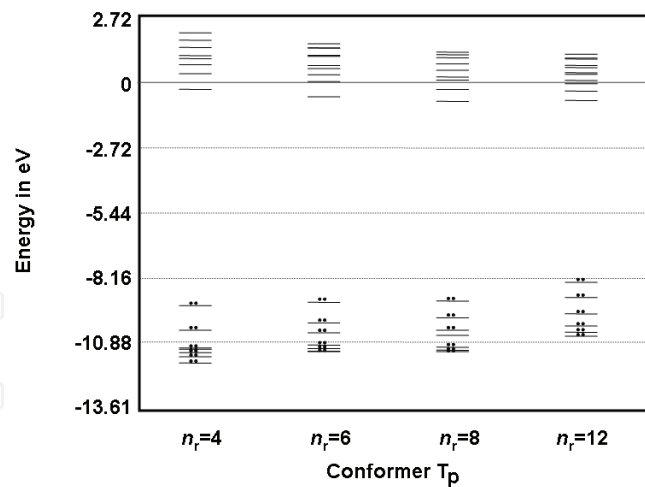


Fig. 5. Electronic states distribution for the valence and conduction bands for the  $T_p$  conformer with  $n_r=4, 6, 8$  and  $12$  carbon atoms forming the structure.

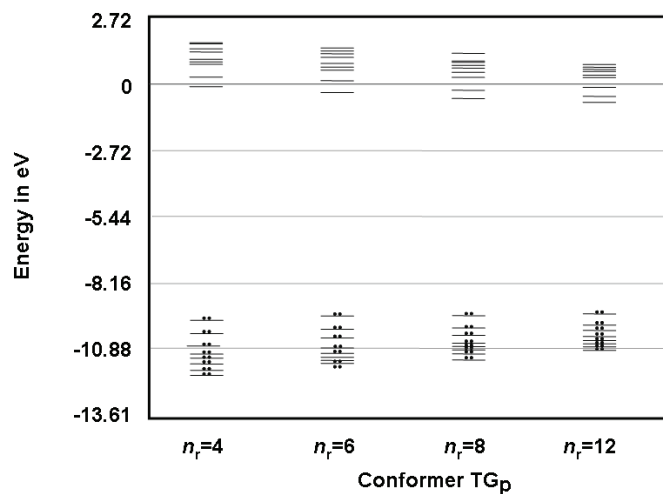


Fig. 6. Electronic states distribution for the valence and conduction bands for the  $TG_p$  conformer with  $n_r=4, 6, 8$  and  $12$  carbon atoms forming the structure.

The analysis of the energy differences among the structural changes obtained along the PES in Figure 2 leads to the values reported in Table 1. Considering only two monomer units, i. e.,  $n_r=4$ , where  $n$  is the total number of carbon atoms in the structure, the computed results indicate that the dipole moment of the  $T_p$  conformation is always higher than the rest of the structural conformations ( $TG_a$  and  $TG_p$ ). This means that the structural arrangement of the  $T_p$  phase promotes an increase in the polarity of the system, as it has been mentioned before. Analyzing the ESP charge distribution for the three cases, charge polarization in PVDF is obtained for the  $T_p$  conformation (*vide* Figure 7), where positive and negative ESP charges arrange in the  $T_p$  conformation. The quantum mechanics calculations of the ESP charge distribution indicate (Figure 4) that the electrical charges are perfectly ordered at the outside part of the molecule, being one side positive and the other negative. In the same way, for the P(VDF-TrFE) system, although the charge is polarized by fluorine atoms being at one outside part completely negative, the other outside part, is mostly positive with exception of the non-symmetric fluorine atom, a sort of contamination. For the P(VDF-CTFE) case, in which a chlorine atom is present in the structure, a charge polarization is also obtained

outside the molecule, exhibiting a negative charge where fluorine atoms are present, but on the other side, there is an alternate charge distribution, being negative at fluorine and chlorine atoms positions and positive at hydrogen atoms positions. The TG's conformational systems do not show a charge polarization or the same split charge distribution (*vide* Figure 4).

So far, the current results for the model's representation give a good description of the system, also in line with previous literature reports. Furthermore, some additional parameters can be presented. On this respect, the  $|\text{HOMO-LUMO}|$  energy difference was also computed. From Table 1, although the  $|\text{HOMO-LUMO}|$  energy gap decreases slowly for the  $T_p$  conformation (in all the studied systems), in previous results for PVDF (Lu et al., 2006), the  $|\text{HOMO-LUMO}|$  energy difference also exhibits a decrease, being highly notorious for the  $T_p$  conformer in P(VDF-CTFE). It decrease from 9.24 eV in the PVDF to 8.32 eV in the P(VDF-CTFE), whereas for the P(VDF-TrFE) the  $|\text{HOMO-LUMO}|$  energy difference is between them, about 9.07 eV. The dipole moment decrease for the PVDF-based materials (P(VDF-TrFE) and P(VDF-CTFE)) being the higher dipole moment for the PVDF (*vide* Table 1). Even so, among the different structures, the  $T_p$  phases present the highest values in the dipole moment with respect to TG's phase structures, no matter if PVDF or PVDF-based materials are.

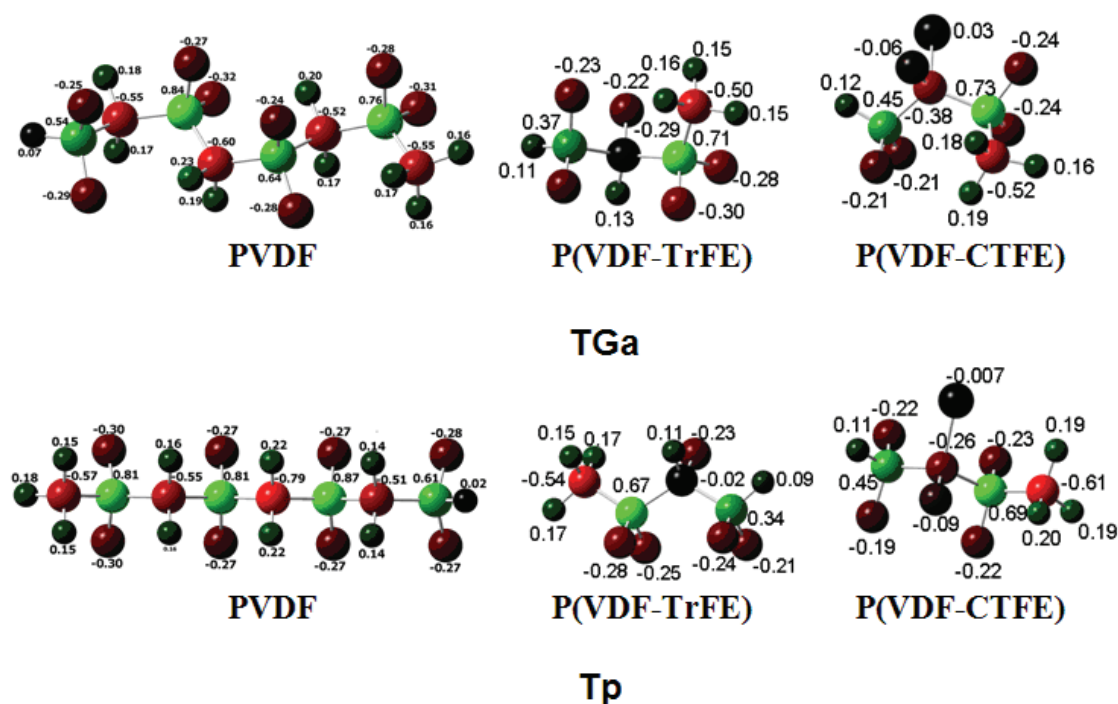


Fig. 7. ESP charge representation for  $TG_a$  and  $T_p$  of the representative model of the different materials, namely, PVDF, P(VDF-TrFE) and P(VDF-CTFE). Negative charge values are in red, positive charge values are in dark green and the larger positive charges are depicted in light green.

When the chain is enlarge for PVDF and P(VDF-CTFE) as a composition of 85 mol % of VDF and 15 mol % of CTFE, as can be seen in the Figure 8, the dipole moment keep similar behavior as in the two monomer units. In this case, for the PVDF in a  $T_p$  phase is 12.6 D, for the P(VDF-CTFE) in  $TG_a$  phase is about 8.95 D and for P(VDF-CTFE) in  $T_p$  phase is 11.32 D.

Analyzing the ESP charge distribution for the three last cases, charge polarization in PVDF is obtained for the  $T_p$  conformation (*vide* Figure 8a), where positive and negative ESP charges arrange in the  $T_p$  conformation. The quantum mechanics calculations of the ESP charge distribution indicate (Figure 8a) that the electrical charges are perfectly ordered at the outside part of the molecule, being one side positive and the other negative. For the P(VDF-CTFE) case, in which a chlorine atom is present in the structure, a charge polarization is also obtained outside the molecule, exhibiting a negative charge where fluorine atoms are present, contrary to obtained when only two monomers are taken into account, *vide* Figure 7 and 8c. The  $TG_a$  conformational system for P(VDF-CTFE) as a composition of 85 mol % of VDF and 15 mol % of CTFE, do not show a charge polarization or the same split charge distribution (*vide* Figure 8b), as it is expected.

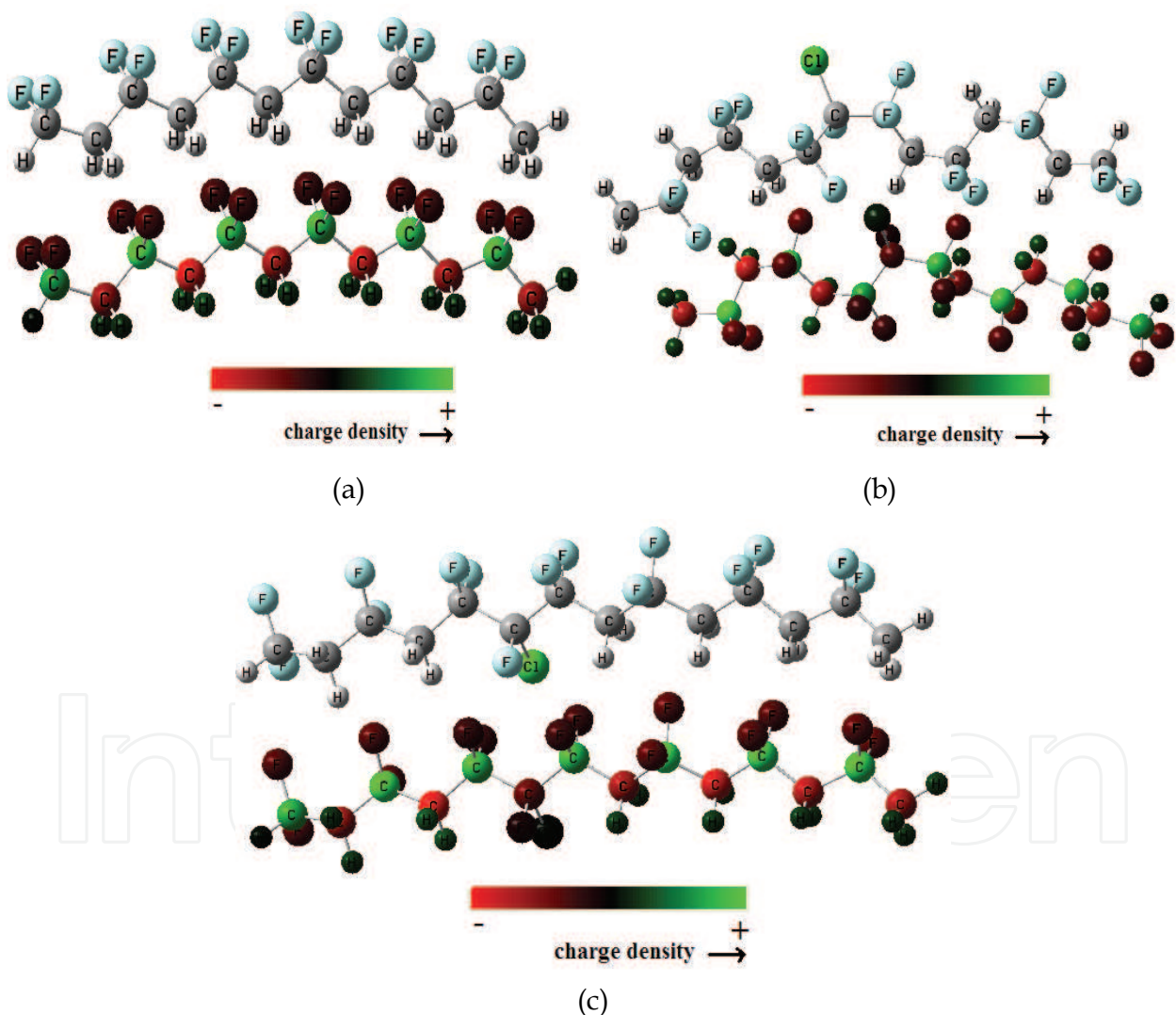


Fig. 8. Geometrical and schematic ESP charge distribution for a representative models for of the different materials, namely, (a)  $T_p$  phase of PVDF; (b)  $TG_a$  phase of P(VDF-CTFE) and (c)  $T_p$  phase of P(VDF-CTFE). P(VDF-CTFE) as a composition of 85 mol % of VDF and 15 mol % of CTFE. Negative charge values are in red, positive charge values are in dark green and the larger positive charges are depicted in light green.

For the system which contain a sort of contamination of fluoride and chlorine atom in the PVDF system to generate the P(VDF-CTFE) as a composition of 85 mol % of VDF and 15 mol % of CTFE, composition studied here, it does not has a strongly effect over the charge polarization for the  $T_p$  phase, but according to the vibrational frequencies obtained for the both phases  $T_p$  and  $TG_a$ - P(VDF-CTFE), the presence of the chlorine atom in the structure gives not too much flexibility to the chain neighboring to it. In fact, as chlorine atom is heavier than fluorine or hydrogen atoms, it anchors the molecule and restricts the mechanic movement. Maybe this special factor gives different properties to the copolymer with respect to PVDF system.

#### 4. Conclusions

Ferroelectric materials are commonly used in electronic devices taking advantage of, for instance, their piezoelectricity, electricity storage capacity and sensing ability. The actual operability of these materials is based on the charge polarization, which is basically due to the energy associated to electron mobility. The fundamentals of PVDF-based materials have gained more and better understanding in recent years. The key for this advancement, from an experimental point of view, is based on the new methods and techniques that look for the interpretation of structural and composition changes of the polymer through improvement of instrumental sensitivity. Likewise, more efficient computational software and modern hardware allow performing complex theoretical calculations to simulate the local and overall chemical phenomena taking into account as many atoms as necessary to obtain reliable results. Quantum-chemical calculations performed using Density functional Theory yield deep understanding on the electronic-structure relationships from fundamentals with well-suited description of the phase transition phenomena.

Dealing with PVDF-based materials model design, the quantum mechanics calculations of the energetics and structures corresponding to the different structural conformations for the PVDF, P(VDF-TrFE) and P(VDF-CTFE) units show that the  $T_p$  conformation is energetically stabilized even with a chlorine substituent. The changes in the molecular arrangement associated to  $T_p$ ,  $TG_a$  or  $TG_p$  conformations lead to significant changes in shape and electrical-chemical properties. A larger dipole moment and spatial charge polarization were obtained for the all-trans  $T_p$  molecular structure, being more ordered in the PVDF system, which can be obtained by accumulative motion of the neighboring groups through large-scale T-G conformational changes. The molecular model shows that the energy barriers among the different structural conformations are not too high, allowing to switch among them with a relatively low energy supply, more easily for P(VDF-TrFE), according to the computed results. The interphase mobility among the different conformations is an important property for actuators. All these additive properties of the  $T_p$  structure model may produce a ferroelectric material when the system size scales up to a polymer crystal.

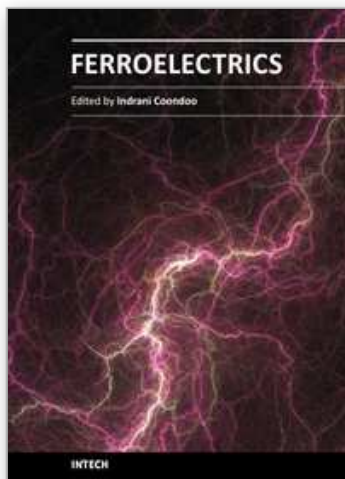
#### 5. References

- ABINIT. The ABINIT programs are a common project of the Universite' Catholique de Louvain, Corning Inc. and other contributors (see <http://www.abinit.org>).
- ABINIT-P. For a description of the ABINIT project, Gonze X, Beuken JM, Caracas R, Detraux F, Fuchs M, Rignanese GM, et al. *Comput Mater Sci* 2002;25:478e92; Gonze X,

- Rignanese GM, Verstraete M, Beuken JM, Pouillon Y, Caracas R, et al. *Z Kristallogr* 2005;220:558e62.
- A. D. Becke. (1993). Density-functional thermochemistry. III. The role of exact exchange, *J. Chem. Phys.* Vol. 98, pp 5648–5653.
- P. Blaha, K.Schwarz and J. Luitz, WIEN97. (1999). A Full Potential Linearized Augmented Plane-Wave Package for Calculating Crystal Properties (Karlheinz Schwarz, Technische Universit<sup>at</sup>Wien, Austria); ISBN 3-9501031-0-4.
- B. H. Brent, K. M. Merz, Jr., and P. A. Kollman. (1990). Atomic charges derived from semiempirical methods. *J. Comput. Chem.* Vol. 11, pp 431–439.
- M. G. Broahurst, G.T. Davis, J.E. McKinney, R.E. Collins. (1978) Piezoelectricity and pyroelectricity in polyvinylidene fluoride – A model. *J Appl Phys* Vol. 49 No. 10, pp 4992-4992.
- R. Casalini, C. M. Roland. (2001). Highly electrostrictive poly(vinylidene fluoride-trifluoroethylene) networks. *Appl. Phys. Lett.* Vol. 79, pp 2627.
- A Casalini, R.; Roland, C. M. Electromechanical properties of poly(vinylidene fluoride-trifluoroethylene) networks *J. Polym. Sci., Part B: Polym. Phys.* 2002,40, 1975.
- Choi Jaewu, P. A. Dowben, Pebley Shawn, A. V. Bune. S. Ducharme, V. M. Fridkin, S. P. Palto and N. Petukhova. (1998). *Phys. Rev. Lett.*, Vol. 80. pp 1328.
- B. Chu, X. Zhou, K. Ren, B. Neese, M. Lin, Q. Wang, F. Bauer, Q. M. Zhang- (2006).A Dielectric Polymer with High Electric Energy Density and Fast Discharge Speed. *Science.* Vol. 313, pp 334-336.
- Chun-gang Duan, W. N. Mei, J. R. Hardy, S. Ducharme, Jaewu Choi and P. A. Dowben. (2003). Comparison of the theoretical and experimental band structure of poly(vinylidene fluoride) crystal. *Europhys. Lett.* Vol. 61 No. 1, pp. 81–87.
- G. Cortili, G. Zerbi. (1967). Chain conformations of polyvinylidene fluoride as derived from its vibrational spectrum. *Spectrochim Acta.* Vol. 23A pp 285-299.
- A. Cuán and C. M. Cortés-Romero. (2010) Theoretical investigations of structural parameters contribution on zeolitic materials and its interaction with model molecules. *Molecular Systems: Theory and Modeling*, Editor(s) F. Jiménez-Cruz and J. L. García-Gutiérrez, ISBN 978-81-7895-391-5, Under Release.
- D. Das, S.L. Whittenburg. (1999). Performance of the hybrid density functionals in the determination of the geometric structure, vibrational frequency and singlet-triplet energy separation of CH<sub>2</sub>, CHF, CF<sub>2</sub>, CCl<sub>2</sub> and CBr<sub>2</sub>. *J of Molecular Structure (Theochem)* Vol. 492 pp 175–186.
- B. Daudin, M. Dubus. (1987). Effects of electron irradiation and annealing on ferroelectric vinylidene fluoride-trifluoroethylene copolymers. *J. Appl. Phys.* Vol. 62, pp 994.
- E. M. Evleth, E. Kassab, and L. R. Sierra (1994). Calculation of the Exchange Mechanism of D<sub>2</sub> and CD<sub>4</sub> with a Zeolite Model. *J. Phys. Chem.* Vol. 98, pp 1421.
- B. L Farmer, A. J Hopfinger. and J. B.Lando. (1972) Effect of trifluoroethylene monomers on molecular conformation of poly (vinylidene fluoride-trifluoroethylene) copolymer. *J. Appl. Phys.* Vol. 43 pp 4293.
- P. J. Feibelman. (1987). Force and total-energy calculations for a spatially compact adsorbate on an extended, metallic crystal surface. *Phys. Rev. B.* Vol. 35, pp 2626.
- GAUSSIAN (1995) M. J. Frisch, G. W. Trucks, H. B. Schlegel, P. M. W. Gill, B. G. Johnson, M. A. Robb, J. R. Cheeseman, T. Keith, G. A. Petersson, J. A. Montgomery, K. Raghavachari, M. A. A I. Laham, V. G. Zakrzewski, J. V. Ortiz, J. B. Foresman, J.

- Cioslowski, B. B. Stefanov, A. Nanayakkara, M. Challacombe, C. Y. Peng, P. Y. Ayala, W. Chen, M. W. Wong, J. L. Andres, E. S. Replogle, R. Gomperts, R. L. Martin, D. J. Fox, J. S. Binkley, D. J. Defrees, J. Baker, J. P. Stewart, M. Head-Gordon, C. Gonzalez, J. A. Pople, Gaussian 94, Revision D.4, Gaussian, Inc., Pittsburgh, PA.
- Q. Gao, J. I. Scheinbeim. (2000). Dipolar Intermolecular Interactions, Structural Development, and Electromechanical Properties in Ferroelectric Polymer Blends of Nylon-11 and Poly(vinylidene fluoride). *Macromolecules*. Vol. 33, pp 7564.
- A. Gómez-Zaravaglia, and R. Fausto. (2004). Self-Aggregation in Pyrrole: Matrix Isolation, Solid State Infrared Spectroscopy, and DFT Study. *J. Phys. Chem. A*. Vol. 108, pp 6953.
- R. Hasegawa, Y. Takahashi, Y. (1972) Chatani and H. Tadokoro, Molecular conformation and packing of poly(vinylidene fluoride). Stability of three crystalline forms and the effect of high pressure *Polym. J.* Vol. 3, pp 591-605.
- B. J. Jungnickel. (1999). Poly(vinylidene fluoride) (overview). In: J.C. Salamone, editor. *Polymeric materials handbook*. New York: CRC Press Inc; pp. 7115-7122.
- N. Karasawa and W. A. Goddard III. (1992). Force, fields, structures and properties of poly(vinylidene fluoride) crystals, *Macromolecules*. Vol. 25 pp7268.
- H. Kawai. (1969) The piezoelectricity of poly(vinylidene fluoride). *Jpn. J. Appl. Phys.* Vol. 8, pp 975.
- M. Kobayashi, K. Tashiro, H. Tadokoro.(1975). Molecular Vibrations of Three Crystal Forms of Poly(vinylidene fluoride). *Macromolecules*. Vol 8, pp 158-171.
- J. B. Lando, H. G. Olf and A. Peterlin. (1966) NMR and X-ray determination of the structure of poly(vinylidene fluoride). *J. Polym. Sci.* Vol. 4, pp 941.
- S. B. Lang, S. Muensit. (2006). Review of some lesser-known applications of piezoelectric and pyroelectric polymers. *Appl. Phys. A* Vol. 85, pp 125-134.
- C. Lee, W. Yang, R.G. Parr. (1988). Development of the Colle-Salvetti correlation-energy formula into a functional of the electron density. *Phys. Rev. B*. Vol. 37, pp 785-789.
- A. J. Lovinger. (1982) Annealing of poly(vinylidene Fluoride) and formation of a fifth phase *Macromolecules*. Vol. 15 pp40-44.
- A. Lovinger. (1983). Ferroelectric polymers. *J. Science* Vol. 220, pp 1115.
- A. J. Lovinger. (1985). Polymorphic transformations in ferroelectric copolymers of vinylidene fluoride induced by electron irradiation. *Macromolecules*. Vol. 18, pp 910-918.
- Y. Lu, J. Claude, Q. M. Zhang, Q. Wang. (2006). Microstructures and Dielectric Properties of the Ferroelectric Fluoropolymers Synthesized via Reductive Dechlorination of Poly(vinylidene fluoride-co-chlorotrifluoroethylene)s, *Macromolecules*. Vol. 39, pp 6962-6968.
- N. I. Makarevich, V. N. Nikitin. (1965). Study of the structure of the  $\alpha$ - and  $\beta$ -forms of polyvinylidene fluoride. *Polym Sci (USSR)*. Vol. 7. Pp 1843-1849.
- H. S. Nalwa. (1995). *Ferroelectric Polymers: Chemistry, Physics, and Applications* (Marcel Dekker, New York, Basel, Hong Kong) pp. 895.
- J. B. Nicholas, A. J. Hopfinger, I L. Eton, and , F. R. Trow. (1991). Molecular modeling of zeolite structure. 2. Structure and dynamics of silica sodalite and silicate force field *J. Am. Chem. Soc.* Vol. 113, pp 4792

- J. B. Nicholas. (1997). Density functional theory studies of zeolite structure, acidity, and reactivity. *Topics in Catalysis*. Vol. 4, pp 157.
- J. Nicholas, T. Ramer, K. Marrone, A. Stiso. (2006). Structure and vibrational frequency determination for a-poly(vinylidene fluoride) using density-functional theory. *Polymer*. Vol. 47, pp7160-7165.
- OPIUM. For OPIUM pseudopotential generation programs, see <http://opium.sourceforge.net>.
- E. Ortiz, A. Cuán, C. Badillo, C. M. CortésRomero, Q. Wang and L. Noreña. (2009) Electronic properties of poly(vinylidene fluoride): A Density Functional Theory Study. *Molecular Simulation*. Vol. 35: No. 6, pp 477 -482
- E. Ortiz, A. Cuán, C. Badillo, C. M. Cortés-Romero, Q. Wang, L. Noreña. (2010). DFT Study of Ferroelectric Properties of the Copolymers: Poly(vinylidene fluoride-trifluoroethylene) and Poly(vinylidene fluoride-chlorotrifluoroethylene) *International Journal of Quantum Chemistry*, Vol. 110, pp 2411-2417
- J. P. Perdew, K. Burke, M. Ernzerhof. (1996). Generalized Gradient Approximation Made Simple *Phys Rev Lett*. Vol.77. Pp 3865-3868.
- A. M. Rappe, K. M. Rabe, E. Kaxiras, J. D. Joannopoulos. (1990). Optimized pseudopotentials. *Phys Rev B*. Vol. 41,pp 1227-1230.
- P. A. Schultz, SeqQuest Electronic Structure Code (Sandia National Laboratories, 2002).
- L. R. Sierra, E. Kassab, and E. M. Evleth. (1993). Calculation of hydroxymethylation of a zeolite model *J. Phys. Chem*. Vol. 97, pp 641-646.
- H. Su, A. Strachan, and W. A. Goddard III. (2004). Density functional theory and molecular dynamics studies of the energetics and kinetics of electroactive polymers: PVDF and P(VDF-TrFE). *Phys Rev B*. Vol. 70, pp 64101
- K. Tashiro, S.Nishimura, M.Kobayashi. (1988). Thermal contraction and ferroelectric phase transition in vinylidene fluoride-trifluoroethylene copolymers. An effect of tensile stress along the chain axis *Macromolecules*. Vol. 21, pp 2463.
- K. Tashiro, Y. Abe, and M. Kobayashi. (1995) Computer simulation of structure and ferroelectric phase transition of vinylidene fluoride copolymers. I. VDF content dependence of the crystal structure. *Ferroelectrics*. Vol. 171, pp 281.
- E. H. Teunissen, A. P. J. Jansen, R. A. van Santen, R. Orlando, R. Dovesi. (1994). Adsorption energies of NH<sub>3</sub> and NH<sub>4</sub><sup>+</sup> in zeolites corrected for the long-range electrostatic potential of the crystal. *J. Chem. Phys*. Vol. 101 pp 5865-5874.
- T. T. Wang, J. M. Herbert, and A. M. Glass. (1988). The Applications of Ferroelectric Polymers (Blackie, Glasgow).
- Z.Y. Wang, H. Q. Fan, K.H. Su, Z.Y. Wen. (2006). Structure and piezoelectric properties of poly(vinylidene fluoride) studied by density functional theory. *Polymer*. Vol. 47, pp 7988-7996.
- T. Wentink, L. J. Willworth, J. P. Phaneuf. (1961). Properties of Polyvinylidene Fluoride. Part II. Infrared Transmission of normal and thermally Decomposed Polymer. *J Polym Sci*. Vol. 55, pp 551-562.
- Q. M. Zhang, V. Bharti, X. Zhao. (1998). Giant Electrostriction and Relaxor Ferroelectric Behavior in Electron-Irradiated Poly(vinylidene fluoride-trifluoroethylene) Copolymer. *Science* Vol. 280, pp 2102.



## **Ferroelectrics**

Edited by Dr Indrani Coondoo

ISBN 978-953-307-439-9

Hard cover, 450 pages

**Publisher** InTech

**Published online** 14, December, 2010

**Published in print edition** December, 2010

Ferroelectric materials exhibit a wide spectrum of functional properties, including switchable polarization, piezoelectricity, high non-linear optical activity, pyroelectricity, and non-linear dielectric behaviour. These properties are crucial for application in electronic devices such as sensors, microactuators, infrared detectors, microwave phase filters and, non-volatile memories. This unique combination of properties of ferroelectric materials has attracted researchers and engineers for a long time. This book reviews a wide range of diverse topics related to the phenomenon of ferroelectricity (in the bulk as well as thin film form) and provides a forum for scientists, engineers, and students working in this field. The present book containing 24 chapters is a result of contributions of experts from international scientific community working in different aspects of ferroelectricity related to experimental and theoretical work aimed at the understanding of ferroelectricity and their utilization in devices. It provides an up-to-date insightful coverage to the recent advances in the synthesis, characterization, functional properties and potential device applications in specialized areas.

### **How to reference**

In order to correctly reference this scholarly work, feel free to copy and paste the following:

Ortiz Elba, Cuan Angeles, Noreña Luis, Cortes- Romero Carlos and Wang Qing (2010). Quantum Chemical Investigations of Structural Parameters of PVDF-based Organic Ferroelectric Materials, *Ferroelectrics*, Dr Indrani Coondoo (Ed.), ISBN: 978-953-307-439-9, InTech, Available from:

<http://www.intechopen.com/books/ferroelectrics/quantum-chemical-investigations-of-structural-parameters-of-pvdf-based-organic-ferroelectric-material>

**INTECH**  
open science | open minds

### **InTech Europe**

University Campus STeP Ri  
Slavka Krautzeka 83/A  
51000 Rijeka, Croatia  
Phone: +385 (51) 770 447  
Fax: +385 (51) 686 166  
[www.intechopen.com](http://www.intechopen.com)

### **InTech China**

Unit 405, Office Block, Hotel Equatorial Shanghai  
No.65, Yan An Road (West), Shanghai, 200040, China  
中国上海市延安西路65号上海国际贵都大饭店办公楼405单元  
Phone: +86-21-62489820  
Fax: +86-21-62489821

© 2010 The Author(s). Licensee IntechOpen. This chapter is distributed under the terms of the [Creative Commons Attribution-NonCommercial-ShareAlike-3.0 License](https://creativecommons.org/licenses/by-nc-sa/3.0/), which permits use, distribution and reproduction for non-commercial purposes, provided the original is properly cited and derivative works building on this content are distributed under the same license.

IntechOpen

IntechOpen